Polypropylene prostheses coated with silver nanoclusters/silica coating obtained by sputtering: Biocompatibility and antibacterial properties

Polypropylene prostheses coated with silver nanoclusters/silica coating obtained by sputtering: biocompatibility and antibacterial properties

Giuliana Muzio[1], Marta Miola[2], Sergio Perero[2], Manuela Oraldi[1], Marina Maggiora[1], Sara Ferraris[2], Enrica Vernè[2], Valentino Festa[3], Federico Festa[3], Rosa Angela Canuto[1], and Monica Ferraris[2]

[1] Department of Clinical and Biological Sciences, University of Turin, Corso Raffaello 30, 10125, Turin, Italy

[2] Department of Applied Science and Technology, Politecnico di Torino, Corso Duca degli Abruzzi 24, 10129 Turin, Italy

[3] Department of Surgical Sciences, University of Turin, Corso Dogliotti 14, 10126 Turin, Italy

Address of corresponding author:

Dr. Marta Miola

Department of Applied Science and Technology

Politecnico di Torino, Corso Duca degli Abruzzi 24, 10129 Turin, Italy

Phone n. +39 0110904717

Fax n. ++39 0110904624

e-mail marta.miola@polito.it

e-mail addresses of authors:

Muzio G, giuliana.muzio@unito.it; Miola M, marta.miola@polito.it; Perero S, sergio.perero@polito.it; Oraldi M, manuela.oraldi@unito.it; Maggiora M, marina.maggiora@unito.it; Ferraris S, sara.ferraris@polito.it; Vernè E, enrica.verne@polito.it; Festa V, valentine.festa@unito.it, Festa F, federico.festa@unito.it; Canuto RA, rosangela.canuto@unito.it; Ferraris M, monica.ferraris@polito.it.

Abstract

With the goal of preventing abdominal infections after implanting prostheses for hernia repair, polypropylene prostheses were coated with a silver nanoclusters-silica composite (Ag/SiO_2) layer, by means of a sputtering process, to confer antibacterial properties.

The Ag/SiO_2 coating was deposited, with good uniformity and adhesion, either onto hernia prostheses (CMC) made of two polypropylene layers (macroporous light mesh and thin transparent film), or onto the mesh layer alone. The coating was optimized to achieve a good balance between antibacterial activity and biocompatibility. Antibacterial activity, fibroblast growth on CMC/mesh layer alone, in the presence/absence of Ag/SiO_2, collagen, and some cytokines involved in inflammation and healing processes, were determined.

Preliminary experiments showed that when both layers of CMC were entirely coated, antibacterial properties were achieved while losing prosthesis biocompatibility. Coating the entire CMC was a complex process, thus for subsequent experiments the mesh layer alone was coated, being the antibacterial properties unaffected by this choice and the mesh the part of CMC exposed to possible infection. With a duty cycle of 1 second over 24 on an Ag target, for 15 minutes deposition time, antibacterial activity, evaluated through the quantitative Colony–Forming Units test, was positive; fibroblasts colonized the coated mesh layer and produced collagen. Cell viability analysis showed that most cells were viable at all experimental times. Moreover, IL-1β and IL-6 decreased, and TGF-β2 increased, in fibroblasts seeded on mesh layer coated with Ag/SiO_2 versus that without Ag/SiO_2.

Ag/SiO_2-coated mesh layers allowed fibroblast growth and activity, without inducing cell death via apoptosis or necrosis and, at the same time, provided antibacterial activity.

1. Introduction

Tissue healing is a complex process involving different cells that produce biological factors and extracellular matrix, and provide mechanical tissue stability [1]. Fibroblasts play a role in tissue repair, and are the primary cell type responsible for collagen synthesis [2]. They contribute to the formation of granulation tissue, and produce modulators of wound healing such as TGF-β [3]. Wound healing can be promoted using biomaterials prepared in the form of a 3D scaffold, which enables appropriate cells to proliferate [4]. Scaffolds are implanted to facilitate healing when defect size, location, tissue type, or genetic abnormalities hinder or prevent fully-autologous regeneration and the return to normal capabilities. Hernia is a case in point. It is characterized by damaged anatomical fascia, and is frequently a secondary complication of abdominal surgery. Exogenous prostheses are used to replace compromised fascia: they can be permanent or reabsorbable, and are made of synthetic polymer meshes or biological tissues. Biological tissues are used in large hernias, when substantial sections of abdominal wall must be reconstructed, while synthetic meshes are preferred for smaller hernias thanks to their malleability and reduced cost [5].

As in wound healing, the implantation of foreign materials induces inflammation and recruits fibroblasts and macrophages, which secrete pro-inflammatory and fibrogenic cytokines [6,7]. Inflammation after mesh positioning is a normal phase in wound healing, as also is the foreign body reaction. It has been shown that all meshes cause initial acute inflammation in proximity to the implant, [8] and that this is associated with early mesh integration. [9,10] Moreover, the degree of inflammation closely correlates with connective tissue formation [8,11]. Recently, meshes have been coated with human fibroblasts (HFBs) or stem cells (MSCs) to improve wound healing, and it has been found that coated meshes, whether synthetic or biological, can be successfully used *in vitro*. MSC coating suppresses mesh-induced IL-1β, IL-6 and VEGF production by macrophages, while HFB coating suppresses IL-1β increasing IL-6 and VEGF [12].

Synthetic mesh has become the standard for most abdominal wall repairs, leading to a considerable reduction in recurrence rates, and in post-operative side effects including, seroma, hematoma and wound breakdown [13-15]. However, the risk of an infection developing around the prosthesis remains a challenge, and the introduction of a prosthesis with antibacterial activity would offer an extremely promising solution in this connection, since it might prevent infection from occurring during implantation or the post-operative period.

Silver is well known for its antibacterial activity, and for its reduced development of resistance, making it of interest as an antibacterial agent to fight both infection and antibiotic resistance. By exploiting a combination of silver's antibacterial action and silica's chemical, mechanical, and thermal stability, an innovative SiO_2-Ag coating suitable for various applications was developed [16-20]. The specific goal of this study was to optimize this coating for application

to synthetic hernia prostheses, in order to give them antibacterial properties. The coating was optimized to achieve a balance among antibacterial action, biocompatibility, and transparency of the final mesh.

2. Materials and Methods

2.1 Preparation and characterization of prostheses

The prostheses comprised two layers of polypropylene: a light macroporous mesh, and a thin transparent film (CMC, Clear Mesh Composite, DIPROMED srl S.Mauro Torinese –Turin, Italy). The mesh layer, facing the parietal side on implantation, is macroporous (88% of porosity, mean pore area 1.8 mm^2, 45 g/m^2); it is made of polypropylene monofilament, 120 μm in diameter, to optimize tissue growth. The film layer, facing the visceral side, consists of non-porous, smooth, transparent polypropylene (Type IV, thickness 70 μm,) to prevent the formation of adhesions on the intestinal side (Figure 1). In designing the device, the mesh was selected of a weave possessing lightness, softness, good stability, and porosity [21]. The polypropylene film was selected for its transparency, enabling blood vessels, nerves, and underlying tissues to be viewed while placing the prosthesis.

The whole CMC, or the mesh layer alone, were sputtered with a layer of Ag nanoclusters-silica. They were coated using a Radio Frequency (RF) magnetron, and co–sputtering SiO_2 and Ag, in order to confer antibacterial properties [16]. Sputtering is one of the methods of Physical Vapor Deposition (PDV); PVD techniques are used to create thin films (from a few nanometers to some microns) upon many different surfaces. The use of thin films has extended into numerous fields, including mechanics, electronics, chemistry, and biomedical applications, exploiting the very interesting properties of a coating when its thickness is reduced to the nanometer scale. Sputtering consists of extracting atoms from a bulk material (the target) using argon ions, obtained by creating a plasma inside a deposition chamber. Very low pressure is created in the deposition chamber (10^{-5} Pa), after which pure argon gas is introduced, maintaining a dynamic pressure of around $10^{-2} \div 10^{-1}$ Pa. A very intense electrical field, applied through the gas, leads the plasma switching–on and consequently the Ar^+ ions formations. The ions, accelerated by the electrical field, collide with the surface of the target(s), and can thus extract atoms or clusters of atoms. The extracted material, flying freely around the deposition chamber, reaches the substrate (the item to be coated) and begins to form the thin film. By controlling the deposition parameters (plasma power, atmosphere, pressure, etc.) it is possible to tailor the morphology and properties of the film. In the case of non-conductive targets (e.g. silica) Radio Frequency (RF) sputtering is used.

The Ag/SiO_2 composite coating tested here had previously been applied onto various substrates for different applications (polymers for aerospace applications, mobile telephones, ocular prostheses, glass, textiles, etc.) [16-20] and has been characterized in terms of morphology, composition, and adhesion. In this study, specific attention was paid to balancing the antimicrobial and biocompatible properties of the resulting coating for biomedical applications.

The coating was obtained by co-sputtering 99.99% pure SiO_2 and 99.99% pure Ag targets. The RF power applied to the silica was 200 W, and 1 W to the Ag target. To tailor the Ag/SiO_2 ratio and avoid Ag excess, the power applied to the Ag was periodically switched on and off throughout the deposition time. The duty cycle is described in Table 1. Due to the more rapid deposition of Ag compared to silica, the plasma over the Ag target was pulsed, as was said above, to avoid the need for excessive reduction of the power applied to the plasma. By controlling the duty cycle, the Ag/SiO_2 ratio in the film can be tailored.

When the entire CMC was coated, the antimicrobial effect was strong, but the device was not biocompatible. In successive experiments, therefore, the mesh layer alone was coated; this is the part of the device that particularly requires antibacterial properties; sputtering parameters were varied, as reported in Table 1.

Prior to deposition, prostheses were cleaned in distilled water at room temperature in an ultrasonic bath. After coating, they were handled under a chemical hood and enclosed in sterile packets, but not further sterilized before microbiological and biological characterization. Deposition parameters that remained unchanged throughout all experiments are listed in Table 2. Morphological-compositional analysis of the coatings was by Field Emission Scanning Electron Microscopy, equipped with Energy Dispersion Spectrometry (FESEM-EDS, Merlin Gemini Zeiss). The chemical and physical characteristics of the antibacterial layer are described in greater detail elsewhere [16–20].

2.2 Microbiological and biological characterization

2.2.1 Microbiological characterization. The antibacterial effect was evaluated using the agar diffusion test [22] (inhibition halo evaluation) in accordance with the National Committee for Clinical Laboratory Standards (NCCLS) [23] and employing *Staphylococcus aureus* strain (ATCC 29213, Rockville, MD, USA). For the inhibition halo test, a 0.5 Mc Farland suspension (containing approximately 1–2x10^8 colonies forming unit (CFU)/ml) was prepared, inoculating *S. aureus* colonies into physiological solution, and checking the turbidity by measuring the Mc Farland index by means of an optical instrument (Phoenix Spec BD McFarland). A portion of this suspension was then spread onto Mueller Hinton agar plates. The CMC or the mesh layer was then placed in contact with the agar and incubated for 24 hours at 35 °C. The antibacterial activity was evaluated by observing the size of the inhibition halo, i.e. the zone in which bacteria did not proliferate around the CMC after incubation.

To verify the capacity of the mesh, coated under 24-1 conditions, to inhibit bacterial adhesion, the quantitative CFU test was employed. Briefly, mesh layer, positioned in a multiwell plate, was covered with 1 ml of bacterial broth containing approximately 5x10^5 CFU. After overnight incubation at 35 °C, the mesh layer was gently washed in physiological solution, and bacteria were detached using a vortex in physiological solution. An aliquot of this solution was serially diluted and spread onto a blood agar plate, which was incubated for 24 hours at 35 °C to allow bacterial growth for

subsequent CFU counting. Both tests were performed in triplicate, and all products used for the analyses were purchased from BD-Becton Dickinson, Franklin Lakes, NJ, USA.

2.2.2 Biological characterization. Human fibroblast BJ cells (ATCC, Rockville, MD, USA), obtained from newborn human foreskin, were cultured (33,000/cm^2) in DMEM medium (high glucose) supplemented with 2 mM glutamine, 1% antibiotic/antimycotic solution, 1% non-essential amino acids, and 10% FBS. Fibroblasts were seeded on polystyrene plastic multiwells, into which the CMC (2.5 cm x 2.5 cm), coated or not, was anchored using biologically-inert sterile stickers; alternatively, non-anchored mesh layers (coated or not) of equal size, were placed in the wells. The fibroblasts seeded on CMC or on mesh layers corresponded to 125,000 total cells. CMC covered the base of the well? completely, thus cells grew only on the CMC. When the mesh was placed in the well, the cells grew on the polypropylene mesh and within its pores. In this case, at the different experimental times, the mesh was removed from the plastic well and put into a new well, where the mesh was treated with trypsin/EDTA to detach the cells growing on the mesh alone. After removing culture medium, CMC colonized by BJ cells were observed under a light-reverted microscope.

Cells were detached from CMC, or from mesh, using trypsin/EDTA (0.25/0.03%). Cell growth was determined by counting cells in a Burker chamber under a light microscope (Leitz, Wetzlar, HM-LUX, GERMANY); viability was evaluated as lactate dehydrogenase release in the culture medium, and DNA content on fixed cells by cytofluorimetric analysis [24].

To evaluate the production of type I collagen by fibroblasts colonizing CMC or mesh layers, monoclonal anti-collagen 1A1 antibody and the ABC Staining System (Santa Cruz Biotechnology, INC, GERMANY) were used. Briefly, cells were fixed directly in the well with methanol at -20 °C for 5 min and washed with PBS. To block nonspecific binding sites, cells were incubated with 10% blocking serum at room temperature for 20 min. After washing with PBS, cells were incubated with primary antibody for 30 min at room temperature, followed by incubation with biotin-conjugated secondary antibody for 30 min at room temperature. Subsequently, cells were incubated with avidin biotin enzyme reagent for 30 min, washed with deionized water, and incubated with 3 drops of peroxidase substrate for 10 min. Collagen was observed under a light-reverted microscope (Nikon Eclipse TS100).

In BJ cells seeded on the mesh layer, the expression of IL-1β, IL-6, TGF-β2, type I and type III collagen was examined using Real-time polymerase chain reaction (PCR) [25]. Total RNA was extracted from the BJ cells grown on mesh layers, coated or not, using the NucleoSpin RNA II Kit (Macherey-Nagel GmbH & Co. KG, Düren, GERMANY). Real-time PCR was performed with single-stranded cDNA prepared from total RNA (1 μg) using a High-Capacity cDNA Archive kit (Applied Bio Systems, Foster City, CA, USA). The forward (FW) and reverse (RV) primers shown in Table 3 were designed using Beacon Designer® software (Bio-Rad, Hercules, CA, USA). Twenty-five microliters of

a PCR mixture containing cDNA template equivalent 40 ng of total RNA, 5 pmoles each of forward and reverse primers, and 2× IQ SYBR Green SuperMix (Bio-Rad, Hercules, CA, USA) were amplified using an iCycler PCR instrument (Bio-Rad, Hercules, CA, USA) with an initial melt at 95°C for 10 min, followed by 35-40 cycles at 95°C for 40 s, annealing temperature for each primer set for 40 s, and 72°C for 40 s. A final extension of 7 min at 72°C was applied. Each sample was tested in duplicate, and threshold cycle (Ct) values were averaged from each reaction. The change in BJ cells grown on coated mesh layer was defined as the relative expression compared to that of BJ cells grown on non-coated mesh layer, calculated as $2^{-\Delta\Delta Ct}$, where ΔCt = (Ct sample – Ct GAPDH) and ΔΔCt = (ΔCt mesh sputtered - ΔCt mesh not coated).

IL-1β, IL-6 and TGF-β2 were also evaluated in culture medium using commercial ELISA kits (Bender MedSystems GmbH, Vienna, AUSTRIA, Biosource Europe S.A., Nivelles, BELGIUM, Abcam, Cambridge, UK).

Statistical analysis: All data are expressed as means ± S.D. Differences between group means were assessed by analysis of variance followed by a post-hoc Newman-Keuls test or by Student *t* test.

3. Results

3.1 Prosthesis preparation and characterization

The CMCs were sputtered with coatings containing different amounts of Ag, to achieve an optimal balance between antibacterial properties and biocompatibility, while also maintaining film transparency. Different sputtering conditions were tested (Table 1) and the SiO_2/Ag ratio consequently ranged between 32% and 45%. Figure 2 shows, as an example, the FESEM-EDS analysis of coating obtained with 6-2 sputtering conditions (secondary and backscattering electron images). The images show spherical silver nanoclusters closely embedded in the silica matrix during the sputtering process. EDS analysis confirmed the presence of both silver and silica on the surface.

3.2 Microbiological and biological characterization

Sputtered in the 6-2/15 min conditions, CMC produced a thin, irregular inhibition halo; bacteria did not proliferate beneath the CMC, indicating the antibacterial effect was good (Figure 1sa, supplementary material). Sputtered in the 6–2/80 min conditions, the antibacterial activity of the CMC was very high: the specimen created an inhibition halo of about 2 – 3 mm (Figure 3), which was irregular in shape, since the specimen did not adhere fully to the agar. Unfortunately, the cells seeded on the CMC sputtered in the 6–2/80 min conditions were all detached after 7 days of experimental time (Figure 2s in supplementary material). Moreover, the appearance of the coated CMC had altered, becoming brown with poor transparency, and the film was damaged.

With deposition parameters 12–1, BJ cells colonized coated CMC and were alive throughout the experimental period. Figure 4 shows the number of cells grown on coated or non-coated CMC, counted in a Burker chamber, after detaching

them with trypsin from CMC. The cell numbers evaluated at 7 and 21 days of cell culture were compared to the number of cells seeded on the well (at time 0). In the absence of Ag/SiO_2, cell numbers increased by 2.41 and 4.4 times at 7 and 21 days, respectively, over those seeded at time 0. In the presence of Ag/SiO_2(12–1), cell numbers increased by 1.6 and 2.4 times at 7 and 21 days, respectively, over those seeded at time 0. Moreover, the number of cells grown on CMC in the presence of Ag/SiO_2 was smaller than that of cells grown in the absence of Ag/SiO_2.

Differences in cell growth were also evidenced by analysis under light microscope (Figure 5). The figure shows that BJ cells colonized both components of CMC (mesh and film layers) and that their number increased during the experimental period, although cell growth was reduced in the presence of Ag/SiO_2. The size of cells, in the presence of Ag/SiO_2, was larger than that of cells without Ag/SiO_2. The analysis of cell viability, evaluated as LDH release (Table 4) and DNA content (data not reported), showed that the majority of cells were viable at all experimental times. However, using 12-1 sputtering conditions, the antibacterial activity was not present and bacteria proliferated on the CMC surface (Figure 1sb in supplementary material).

To determine the activity of fibroblasts grown on CMC, type I collagen was evaluated (Figure 6) evidencing collagen deposition and no appreciable difference between activity in the presence or absence of Ag/SiO_2 (12-1).

Since preliminary experiments, in which the CMC was entirely coated, failed to detect an Ag concentration conferring antibacterial properties while maintaining prosthesis biocompatibility, it was decided thereafter to sputter the mesh layer alone. This was partly due to the difficulty of finding deposition parameters suitable for the film. It appears likely that the different additives in the film and in mesh layers mean that only the mesh layer can withstand the sputtering deposition parameters 12-1; film sputtered with the same parameters used for the mesh showed widespread superficial damage. It is in any case true that the mesh layer is the only part of this device that effectively requires antibacterial properties, whereas it is important for the film to have the lowest possible adhesion to the viscera. Further, the Ag coating is brownish in color, its intensity depending on the concentration and coating thickness. Since, as was said, transparency is important for the film layer, it is favorable to sputter the mesh layer and not the film.

Using a duty cycle of 1 second over 24 (24–1) on the Ag target, for a total 15 minutes of deposition time (24–1/15), the mesh layer showed antibacterial activity. The count of CFU adhering to the CMC surface demonstrated a reduction in bacterial colony number of two orders of magnitude for sputtered mesh compared to non-sputtered controls (Figure 7).

Figure 8 shows the number of BJ cells on the mesh layers at 14, 21 and 28 days, in the presence or absence of Ag/SiO_2. In the absence of Ag/SiO_2, cells colonized the mesh layers, and had increased by 1.36, 2.05, and 3.04 times, at 14, 21, and 28 days, respectively, compared with cells seeded at time 0. In the presence of the same concentration of Ag/SiO_2, the cell number was lower than that of cells grown in the absence of Ag/SiO_2: cells did not increase at 14 days, but

increased 1.81, and 2.29 times, at 21, and 28 days, respectively. The analysis of cell viability evaluated as LDH release (Table 4) and DNA content (data not reported) showed that the majority of cells were viable at all experimental times.

To determine the activity of fibroblasts seeded on sputtered or non-sputtered mesh layers, collagen production was evaluated by real time PCR and immunohistochemistry (Figures 9 and 10). Evaluation of mRNA content evidenced that, in the presence of Ag/SiO_2, cells expressed more collagen than in its absence; immunohistochemistry analysis showed no appreciable difference in the presence or absence of Ag/SiO_2.

The main aim of using Ag was to induce an antibacterial effect. However, its ability to modulate inflammatory and repair processes was also tested. Figure 11 shows that the IL–1β and IL–6 mRNA decreased in BJ cells seeded on coated mesh layers in comparison with cells seeded on non-coated mesh, at all experiment times. By contrast, the expression of TGF–β2, involved in tissue regeneration, increased at all experiment times. Changes in the expression of cytokines were confirmed by the evaluation of their release in the culture medium (Figure 12).

4. Discussion

Previous *in vitro* studies by the same research group demonstrated the biocompatibility of CMC. It has been shown to be colonized by human fibroblasts BJ [21] and keratinocytes NCTC 2544 [26] and to stimulate the expression of specific activity markers and of factors regulating cell proliferation. Prostheses for hernia repair should also possess antibacterial properties in order to prevent infection after surgery.

Antimicrobial drugs are increasingly ineffective since bacteria develop antibiotic resistance, for example, through the expression of enzymes, which block antibacterial drugs in different ways. Moreover, antibacterial drugs can select resistant bacterial strains [27].

The recent development of nanotechnology may help solve infection problems [28]. Among metal nanoparticles, Ag and its compounds have always been the most interesting and promising candidates, because of their antibacterial properties [29-34]. Various methods can be used for Ag coating: plasma spray, ion beam assisted deposition, magnetron sputtering, micro-arc oxidation, and the sol-gel process [35]. In this research, Radio Frequency (RF) magnetron co–sputtering of SiO_2 and Ag was used. Several different Ag/SiO_2 ratios and duty cycles were tested (Table 1) to determine the quantity of Ag able to confer antibacterial activity to prostheses without affecting their biocompatibility. Sputtering both layers of the CMC created a number of problems: the amount of Ag that maintained cell growth and activity did not confer antibacterial properties (Sputtering condition 12–1/15). By contrast, concentrations that determined antibacterial activity (sputtering conditions 6–2/15 and 6–2/80) caused cell death. In particular, in the latter condition, at 14 days no cells were present on the coated CMC, whereas the number of cells growing on the non-coated CMC was larger than that at 7 days. Moreover, in these conditions, the macroscopic appearance of the CMC was affected, since

the film lost its transparency and was damaged. For these reasons, and because this part of the device is that most exposed to bacterial colonization, only the mesh layer was sputtered thereafter. The film side is manufactured so as to be extremely smooth, avoiding tissue adhesion and adherence, and this property can be maintained if it is left untreated.

After a careful optimization of the process parameters, the sputtering condition 24–1/15 was found to be the most promising one in terms of conferring antibacterial activity, as evidenced by the CFU count. In future research, the test will be repeated using the more efficient sonication method to detach bacteria from the CMC surface, to confirm the data presented here. Under sputtering condition 24–1/15, BJ cells were able to grow, although to a lesser extent than in the absence of Ag/SiO_2. This was probably due to the fact that the Ag released in the early days inhibited cell growth. For longer incubation times, the same percentage of cell growth was observed both in presence and the absence of Ag/SiO_2. Moreover, the majority of fibroblasts were viable and maintained their ability to produce collagen.

As regards the effect of Ag/SiO_2 on inflammation, IL-1β and IL–6 expression was lower in the presence of Ag/SiO_2. Conversely, TGF–β2, which favors fibroblast proliferation and activity, increased. An acute inflammatory process is essential in the early phases of tissue healing [7–11]; this acute inflammation then decreases, and is followed by the production of granulation tissue, specific tissue regeneration, and prosthesis integration. These events are consequent on a decrease in inflammatory cytokines, and an increase in factors inducing cell growth, such as TGF–β2. The results of this research agree with those of previous research evidencing that cytokines, IL–6, IL–1β and TNF–α, levels increased in the culture medium of BJ cells grown on prostheses at the early experimental time, and decreased at subsequent time-points [21].

5. Conclusions

In this study, polypropylene prostheses for hernia repair were coated with silver nanoclusters-silica composite (Ag/SiO_2) layer by means of a sputtering technique, to impart antibacterial properties.

The sputtering process parameters were tailored to balance antibacterial activity and biocompatibility of the prosthesis. In the early experiments, the coating was applied to both the macroporous light mesh and the thin transparent film of the CMC, Thereafter, it was deposited only on the mesh. The Ag/SiO_2 coating appeared uniform both onto hernia prosthesis and onto the mesh layer alone.

When the entire CMC prosthesis was coated with the amount of Ag/SiO_2 that could confer excellent antibacterial properties, biocompatibility was lost. Conversely, when the mesh layer alone was coated, the prosthesis maintained its transparency, showed good antibacterial properties, and biocompatibility: fibroblasts colonized the coated mesh layers and produced collagen. Cell viability measurements showed that the majority of cells were viable at all experimental

times. Moreover, a decrease of IL–1β and IL–6 and an increase of TGF–β2 were observed in fibroblasts seeded on the mesh layer coated with Ag/SiO_2 compared with mesh layers without Ag/SiO_2.

6. **Conflict of interest**: GM declares no conflict of interest; SP declares no conflict of interest; MM declares no conflict of interest; MO declares no conflict of interest; EP declares no conflict of interest; SF declares no conflict of interest; EV declares no conflict of interest; VF declares no conflict of interest; FF declares no conflict of interest; RAC declares no conflict of interest; MF declares no conflict of interest.

7. Acknowledgements.

This research was supported by grants from Regione Piemonte CIPE 2007 – Converging Technologies, Italy, and University of Turin, Italy.

The authors thank DIPROMED srl, S.Mauro Torinese –Turin, Italy for providing prostheses, and thank Frances Cooper for revising the manuscript.

8. References

[1] N. Bryan, H. Ahswin, N. Smart, et al., The in vivo evaluation of tissue-based biomaterials in a rat full-thickness abdominal wall defect model. J Biomed Mater Res B Appl Biomater, 102(4) (2013) 709-20 doi: 10.1002/jbm.b.33050.

[2] B. Hinz, G. Gabbiani, Mechanisms of force generation and transmission by miofibroblast. Curr Opin Biotechnol 14 (2003) 538–546.

[3] K.A. Bielefeld, S. Amini-Nik, B.A. Alman Cutaneous wound healing: recruiting developmental pathways for regeneration. Cell Mol Life Sci 70 (2013) 2059-2081.

[4] D. Williams, To engineer is to create: The link between engineering and regeneration, Trends Biotechnol 24 (2006) 4–8.

[5] Y. Bilsel, I. Abci, The search for ideal hernia repair; mesh, materials and types. Int J Surg 10 (2012) 317–321.

[6] M. Kelly, M. Kolb, P. Bonnaiud, et al., Re-evaluation of fibrogenetic cytokines in lung fibrosis. Curr Pharm Des 9 (2003) 39–49.

[7] L. Tang, J.W. Eaton, Natural responses to unnatural materials: a molecular mechanism for foreign body reactions. Mol Med 5 (1999) 351–358.

[8] R. Gonzalez, B.J. Ramshaw, Comparison of tissue integration between polyester and polypropylene prostheses in the preperitoneal space. Am Surg 69 (2003) 471–477.

[9] J.M. Bellòn, J. Bujan, L. Contreras, et al., Integration of biomaterials implanted into abdominal wall: Process of scar formation and macrophage response. Biomaterials 16 (1995) 381–387.

[10] Y. Marois, R. Cadi, J. Gourdon, et al., Biostability, inflammatory response and healing characteristics of a fluoropassivated polyester-knit mesh in the repair of experimental abdominal hernias. Artif Organs 24 (2000) 533–543.

[11] B. Klosterhalfen, U. Klinge, V. Schumpelick, Functional and morphological evaluation of different polypropylene-mesh modifications for abdominal wall repair. Biomat. 19 (1998) 2235–2246.

[12] E.E. Sadava, D.M. Krpata, Y. Gao, et al., Wound healing process and mediators: Implications for modulations for hernia repair and mesh integration. J Biomed Mater Res Part A, 102A (2013) 295–302.

[13] G.E. Leber, J.L. Garb, A.I. Alexander, et al., Long-term complications associated with prosthetic repair of incisional hernias. Arch Surg 133 (1998) 378–382.

[14] C.R. Voyles, J.D. Richardson, K.I. Bland, et al., Emergency abdominal wall reconstruction with polypropylene mesh: Short-term benefits versus long-term complications. Ann Surg 194 (1981) 219–223.

[15] J.P. Fischer, J.D. Wink, J.A. Nelson, et al., Among 1,706 cases of abdominal wall reconstruction, what factors influence the occurrence of major operative complications? Surgery 155 (2014) 311-319.

[16] M. Ferraris, S. Perero, M. Miola, et al., Silver nanocluster–silica composite coatings with antibacterial properties. Mater Chem Phys 120 (2010) 123-126.

[17] M. Ferraris, S. Perero, M. Miola, S. Ferraris, G. Gautier, G. Maina, G. Fucale, E. Verne', Chemical, mechanical and antibacterial properties of silver nanocluster - silica composite coatings obtained by sputtering, Adv Eng Mater 12 (2010) B276-B282.

[18] C. Balagna, S. Perero, S. Ferraris, M. Miola, G. Fucale, C. Manfredotti, A. Battiato, D. Santella, E. Vernè, E. Vittone, M. Ferraris, Antibacterial coating on polymer for space application, Mat Chem Phis 135 (2012): 714-722

[19] S. Ferraris, S. Perero, M. Miola, E. Vernè, A. Rosiello, V. Ferrazzo, G. Valletta, J. Sanchez, M. Ohrlander, S. Tjörnhammar, M. Fokine, F. Laurell, E. Blomberg, S. Skoglund, I. Odnevall Wallinder, M. Ferraris, Chemical, mechanical and antibacterial properties of silver nanocluster/silica composite coated textiles for safety systems and aerospace applications, Appl. Surf. Sci. 317 (2014) 131–139.

[20] M. Miola, S Perero, S Ferraris, A Battiato, Ch Manfredotti,E Vittone, D Del Vento, S Vada, G Fucale, M Ferraris, Silver nanocluster-silica composite antibacterial coatings for materials to be used in mobile telephones, App. Surf. Sci. 313 (2014) 107–115.

[21] R.A. Canuto, S. Saracino, M. Oraldi, et al., Colonization by human fibroblasts of polypropylene prosthesis in a composite form for hernia repair. Hernia 17 (2013) 241-248.

[22] NCCLS M2-A9 Performance standards for antimicrobial disk susceptibility tests, Approved Standard. 9th edn. NCCLS, Villanova, USA (2003).

[23] G. Muzio, M. Maggiora, M. Oraldi, et al., PPARα and PP2A are involved in the proapoptotic effect of conjugated linoleic acid on human hepatoma cell line SK-HEP-1. Int J Cancer 121 (2007) 2395-2401.

[24] M. Mozzati, G. Martinasso, R. Pol, et al., The impact of plasma rich in growth factors on clinical and biological factors involved in healing processes after third molar extraction. J Biomed Mater Res A 95 (2010) 741-746.

[25] M. Oraldi, S. Saracino, M. Maggiora, et al., Importance of Inverse Correlation Between ALDH3A1 and PPARγ in Tumour Cells and Tissue Regeneration. Chem Biol Interact 19 (2011) 171-176.

[26] F.C. Tenover, Mechanisms of antimicrobial resistance in bacteria. Am J Med 119 (2006) S3–S10.

[27] I. Matai, A. Sachdev, P. Dubey, et al., Antibacterial activity and mechanism of Ag-ZnO nanocomposite on S. aureus and GFP-expressing antibiotic resistant E. coli. Colloids Surf B Biointerfaces 115C (2013) 359-367.

[28] J.R. Morones, J.L. Elechiguerra, A. Camacho, et al., The bactericidal effect of silver nanoparticles. Nanotechnology 16 (2005) 2346–2353.

[29] J.S. Kim, E. Kuk, K.N. Yu, et al., Antimicrobial effects of silver nanoparticles. Nanomed Nanotechnol Biol Med 3 (2007) 95–101.

[30] M. Bosetti, A. Massè, E. Tobin, et al., Silver coated materials for external fixation devices: *In vitro* biocompatibility and genotoxicity. Biomaterials 23 (2002) 887–892.

[31] S. Saint, J.G. Elmore, S.D. Sullivan, et al., The efficacy of silver alloy-coated urinary catheters in preventing urinary tract infection: A meta-analysis. Am J Med 105 (1998) 236–241.

[32] R.O. Darouiche, Anti-infective efficacy of silver-coated medical prostheses. Clin Infect Dis 29 (1999) 1371–1377.

[33] V. Alt, T. Bechert, P. Steinrucke, et al., An *in vitro* assessment of the antibacterial properties and cytotoxicity of nanoparticulate silver bone cement. Biomat. 25 (2004) 4383–4391.

[34] J. Qu, X. Lu, D. Li, et al., Silver/hydroxyapatite composite coatings on porous titanium surfaces by sol-gel method. J Biomed Mater Res B Appl Biomater 9 (2011) 40-48.

Figure captions

Fig. 1

The prosthesis (CMC) comprising two polypropylene layers, one macroporous light mesh and one thin transparent film.

Fig.2

FESEM micrographs (a) secondary electrons, (b) backscattering electrons and (c) EDS analysis of prosthesis sputtered under 6-2 conditions.

Fig. 3

Inhibition halo in the presence of prosthesis sputtered under 6-2 conditions.

Fig. 4

Growth of fibroblasts BJ on CMC not sputtered and sputtered with Ag/SiO_2.

Data are means ± S.D. of 4 experiments. Means with different letters are significantly different from one another ($p<0.05$) as determined by analysis of variance followed by the post-hoc Newman-Keuls test.

CMC, Clear Mesh Composite not sputtered; Ag, CMC sputtered with Ag/SiO_2 (12–1/15)

Fig. 5

Light-microscope analysis of fibroblasts BJ grown on the CMC not sputtered and sputtered with Ag/SiO_2.

CMC, non-sputtered Clear Mesh Composite; Ag, CMC sputtered with Ag/SiO_2 (12–1/15)

Fig. 6

Immunohistochemistry analysis of type I collagen produced by fibroblasts BJ grown on CMC not sputtered and sputtered with Ag/SiO_2. CMC, non-sputtered Clear Mesh Composite; Ag, CMC sputtered with Ag/SiO_2 (12–1/15)

Fig. 7

Effect of Ag/SiO_2 sputtering (24-1/15) on bacterial colony formation (CFU assay).

Data are means ± S.D. of 3 experiments. Student *t* test: $p < 0.05$.

Fig. 8

Growth of fibroblasts BJ on mesh layer not sputtered and sputtered with Ag/SiO_2.

Data are means ± S.D. of 4 experiments. Means with different letters are significantly different from one another ($p<0.05$) as determined by analysis of variance followed by the post-hoc Newman-Keuls test.

mesh, non-sputtered mesh layer; Ag, mesh layer sputtered with Ag/SiO_2 (24-1/15)

Fig. 9

Types I and III collagen mRNA content in fibroblasts BJ grown on the mesh layer not sputtered and sputtered with Ag/SiO_2.

Values of mRNA content, evaluated at 14, 21 and 28 days, in fibroblasts grown on meshes coated with Ag/SiO_2 (black bar) were referred to those of fibroblasts grown in the absence of Ag, taken as 1 (white bar). Data are means of 2 experiments.

mesh, non-sputtered mesh layer; Ag, mesh layer sputtered with Ag/SiO_2 (24-1/15)

Fig. 10

Immunohistochemistry analysis of type I collagen produced by fibroblasts BJ grown on the mesh layer not sputtered and sputtered with Ag/SiO_2.

mesh, non-sputtered mesh layer; Ag, mesh layer sputtered with Ag/SiO_2 (24-1/15)

Fig. 11

IL-1β, IL-6, and TGF-β2 mRNA content in fibroblasts BJ grown on the mesh layer not sputtered and sputtered with Ag/SiO_2

mRNA content was evaluated at 14, 21 and 28 days. Data are means of 2 experiments. Values of fibroblasts grown on mesh layer coated with Ag/SiO_2 (black bar) were referred to those of fibroblasts grown in the absence of Ag, taken as 1 (white bar).

mesh, non-sputtered mesh layer; Ag, mesh layer sputtered with Ag/SiO_2 (24-1/15)

Fig. 12

IL-1β, IL-6 and TGF-β2 protein content in the culture medium of fibroblasts BJ grown on the mesh layer not sputtered and sputtered with Ag/SiO_2.

Protein content was evaluated at 14, 21 and 28 days. Data are means of 2 experiments. Values of cytokines evaluated in the medium of fibroblasts BJ grown on mesh layer coated with Ag/SiO_2 (black bar) were referred to those of fibroblasts grown in the absence of Ag, taken as 100 % (white bar).

mesh, non-sputtered mesh layer; Ag, mesh layer sputtered with Ag/SiO_2 (24-1/15)

Table 1. Sputtering conditions and summary of the biological performances of coated samples

Deposition Name	Total Deposition Time (minutes)	Film Thickness (nm)	Total Duty Cycle Time (seconds)	Plasma ON period (seconds)	Plasma OFF period (seconds)	Ag/Si ratio %at	Prostheses part covered	Antibacterial activity	Biocompatibility
6 – 2 / 15	15	50 – 100	6	2	4	0.4 ÷ 0.5	Mesh+film	✓	✗
6 – 2 / 80	80	300 – 350	6	2	4	0.4 ÷ 0.5	Mesh+film	✓	✗
12 – 1 / 15	15	50 – 100	12	1	11	< 0.4	Mesh+film	✗	✓
24 – 1 / 15	15	50 – 100	24	1	23	< 0.4.	Mesh only	✓	✓

Table 2. Working gas and vacuum parameters of sputtering process

WORKING GAS/VACUUM PARAMETERS		
Atmosphere:	Ar 100 %	
Vacuum Pressure:	70 (0.7)	µPa (pbar)
Deposition Pressure:	7.5 (7.5)	dPa (µbar)

TABLE 3 Forward and reverse sequences of real-time PCR primers

GENE Accession number	SEQUENCE FW (Forward) RV (Reverse)	Ta No. CYCLES	Product length
GAPDH NM_002046	FW 5'-GTC GGA GTC AAC GGA TTT GG-3' RV 5'-GGG TGG AAT CAT ATT GGA ACA TG-3'	52°C 35 X	142 bp
IL-1β AF043335	FW 5'- GCA CCT TCT TTC CCT TCA TCT TT-3' RV 5'- GCG TGC AGT TCA GTG ATC GTA-3'	52°C 40 X	105 bp
IL-6 M14584	FW 5'- CCA GTA CCC CCA GGA GAA GAT T-3' RV 5'- GTC AAT TCG TTC TGA AGA GGT GAG T-3'	52°C 40 X	78 bp
TGF-β2 NM_003238	FW 5'- GAG TAC TAC GCC AAG GAG GTT TAC A-3' RV 5'- CGA ACA ATT CTG AAG TAG GGT CTG T-3'	52°C 40 X	104 bp
Collagen type I NM_000089	FW 5'- GAG GAA ACT GTA AGA AAG G-3' RV 5'- GTT CCC ACC GAG ACC-3'	58°C 35 X	150 bp
Collagen type III NM_000090	FW 5'- ACT CGC CCT CCT AAT GG- 3' RV 5'- GGC ATG ATT CAC AGA TTC C- 3'	59°C 35 X	148 bp

Ta, annealing temperature

Table 4 Lactate dehydrogenase activity in culture medium of fibroblasts BJ grown on CMC or mesh layer not sputtered or sputtered with Ag/SiO_2

	7 days	14 days
CMC	1.54 ± 0.20	2.81 ± 0.55
CMC + Ag	1.21 ± 0.12	2.40 ± 0.26
Mesh layer	1.60 ± 0.30	3.08 ± 0.54
Mesh layer + Ag	1.42 ± 0.55	2.84 ± 0.31

Data are espressed as nmoles of NADH consumed/min/ml of medium and are means ± S.D. of 3 experiments.

CMC, Clear Mesh Composite not sputtered; Ag, CMC sputtered with Ag/SiO_2 (12–1/15);

mesh, mesh layer not sputtered; Ag, mesh layer sputtered with Ag/SiO_2 (24-1/15).

Figure 1

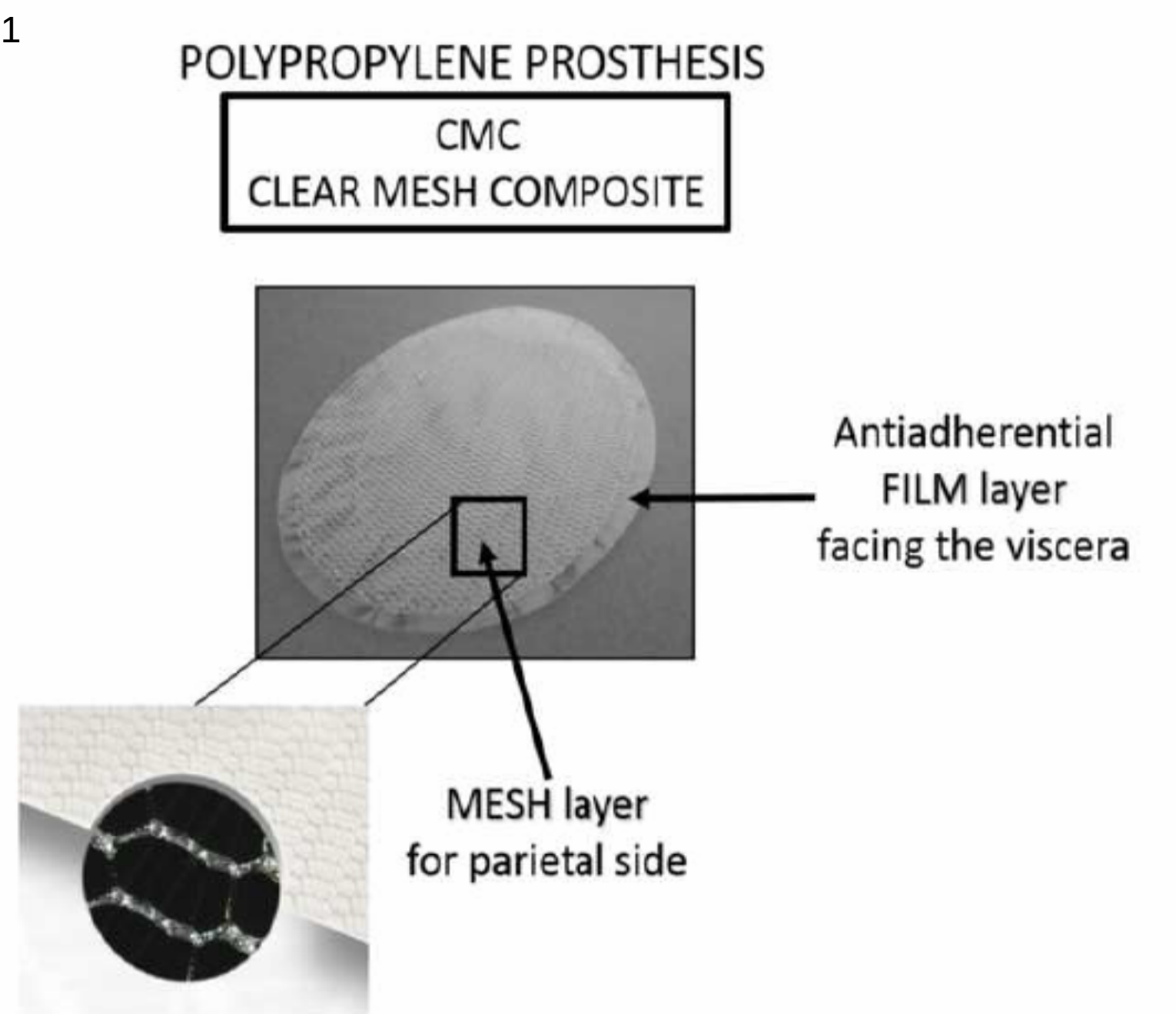
POLYPROPYLENE PROSTHESIS
CMC
CLEAR MESH COMPOSITE
Antiadherential
FILM layer
facing the viscera
MESH layer
for parietal side

Figure 2

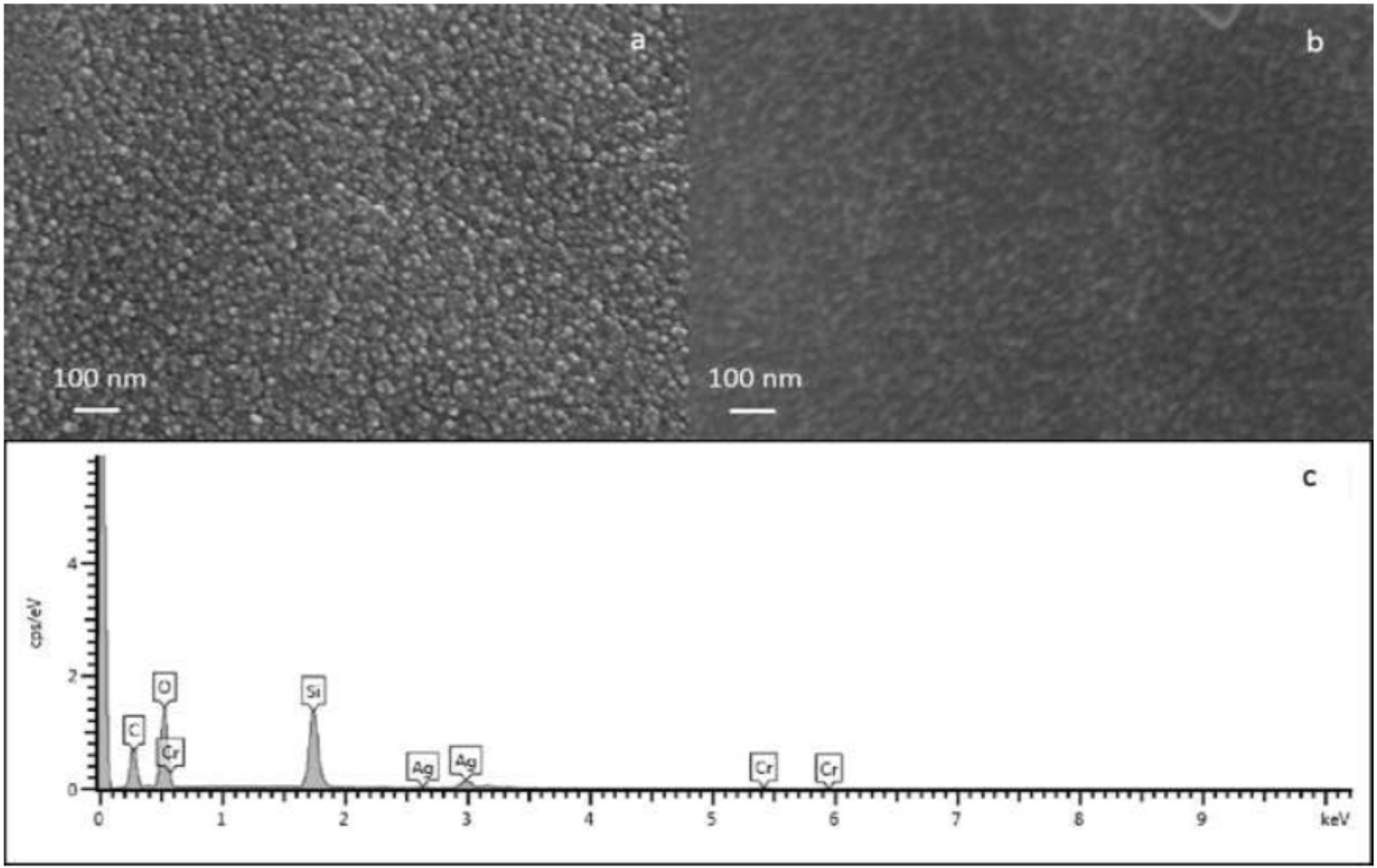

Figure 3

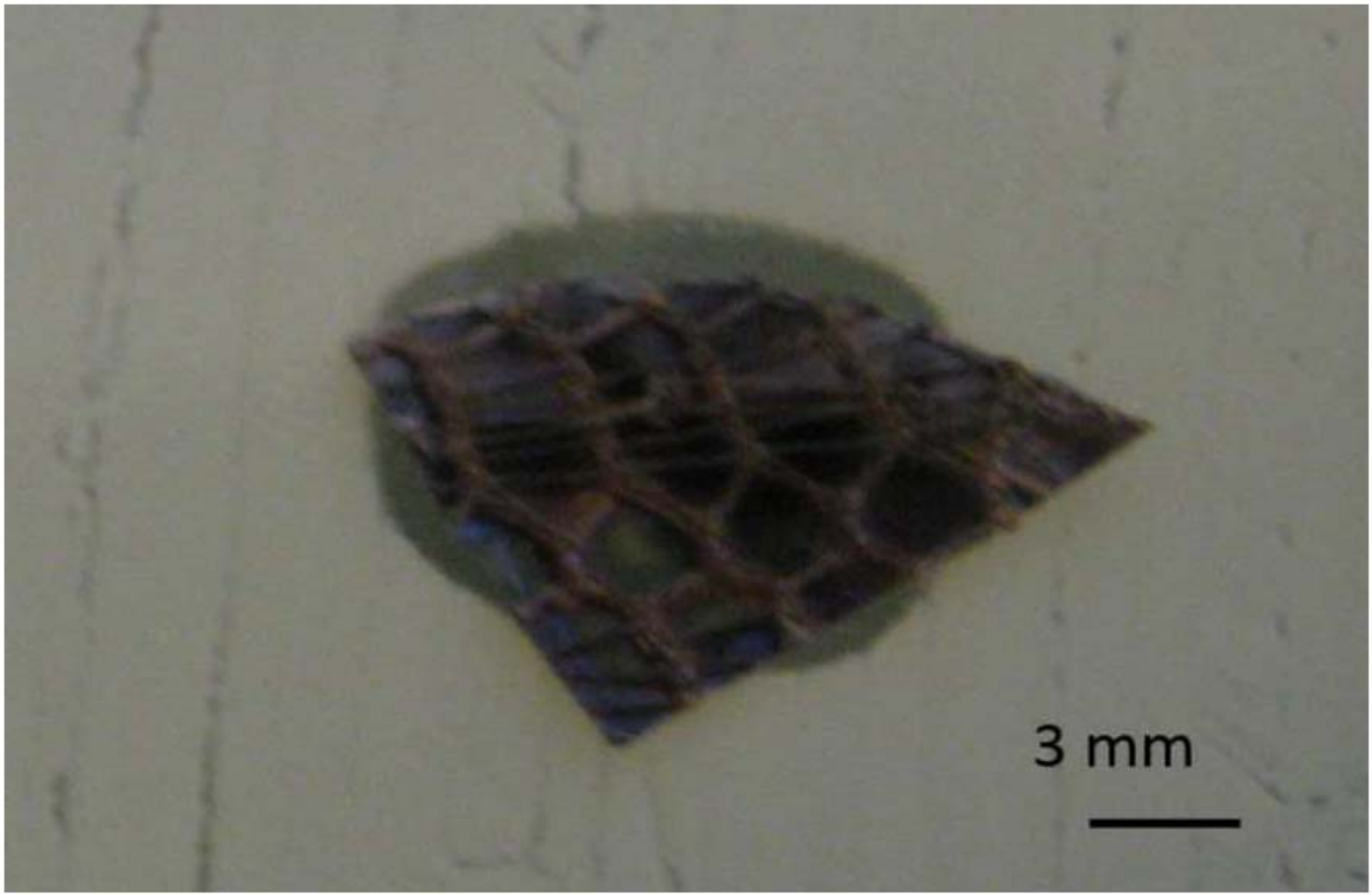

Figure 4

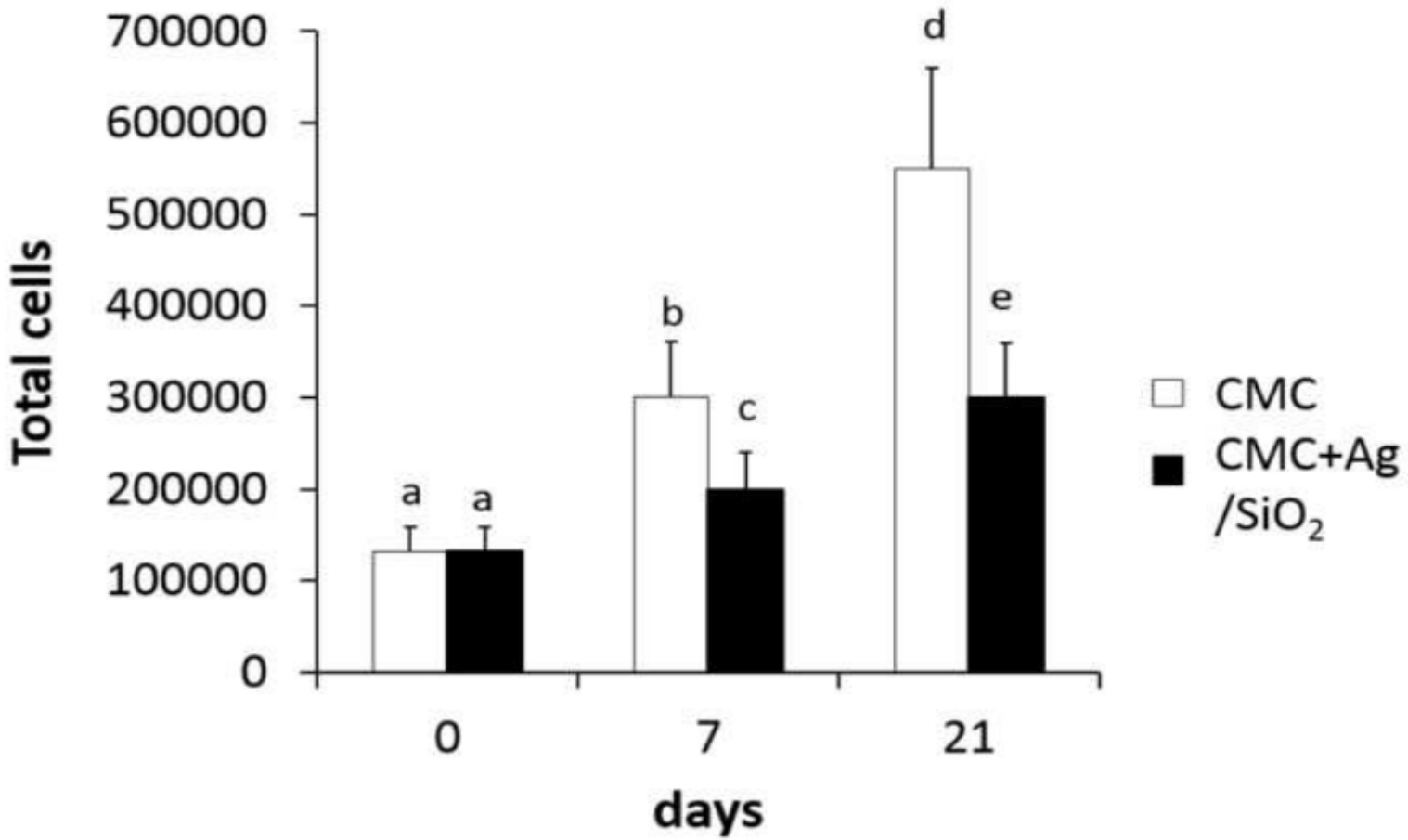
Total cells
700000
600000
500000
400000
300000
200000
100000
0
a
a
b
c
d
e
0
7
21
days
CMC
CMC+Ag /SiO2

Figure 5

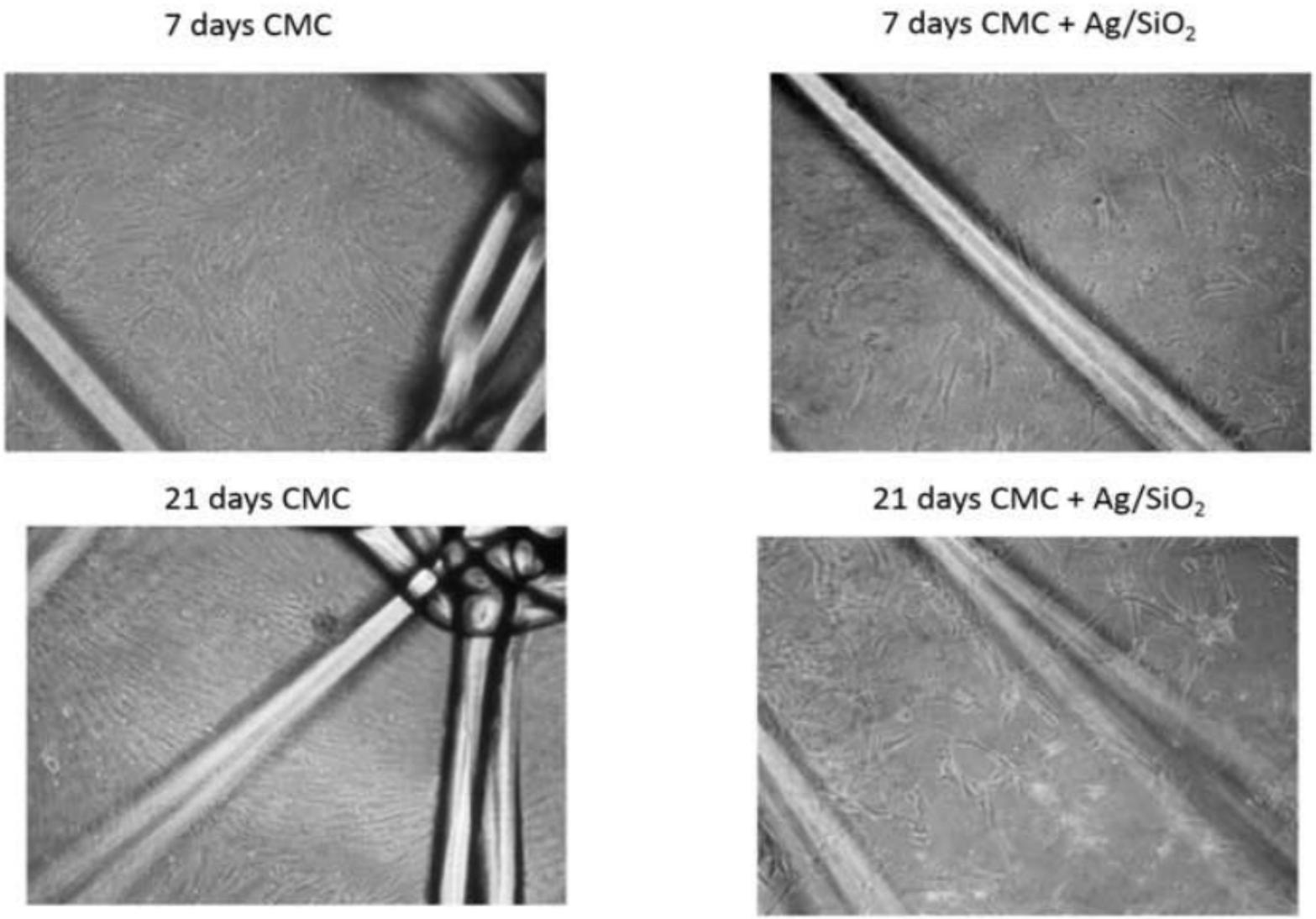

Figure 6

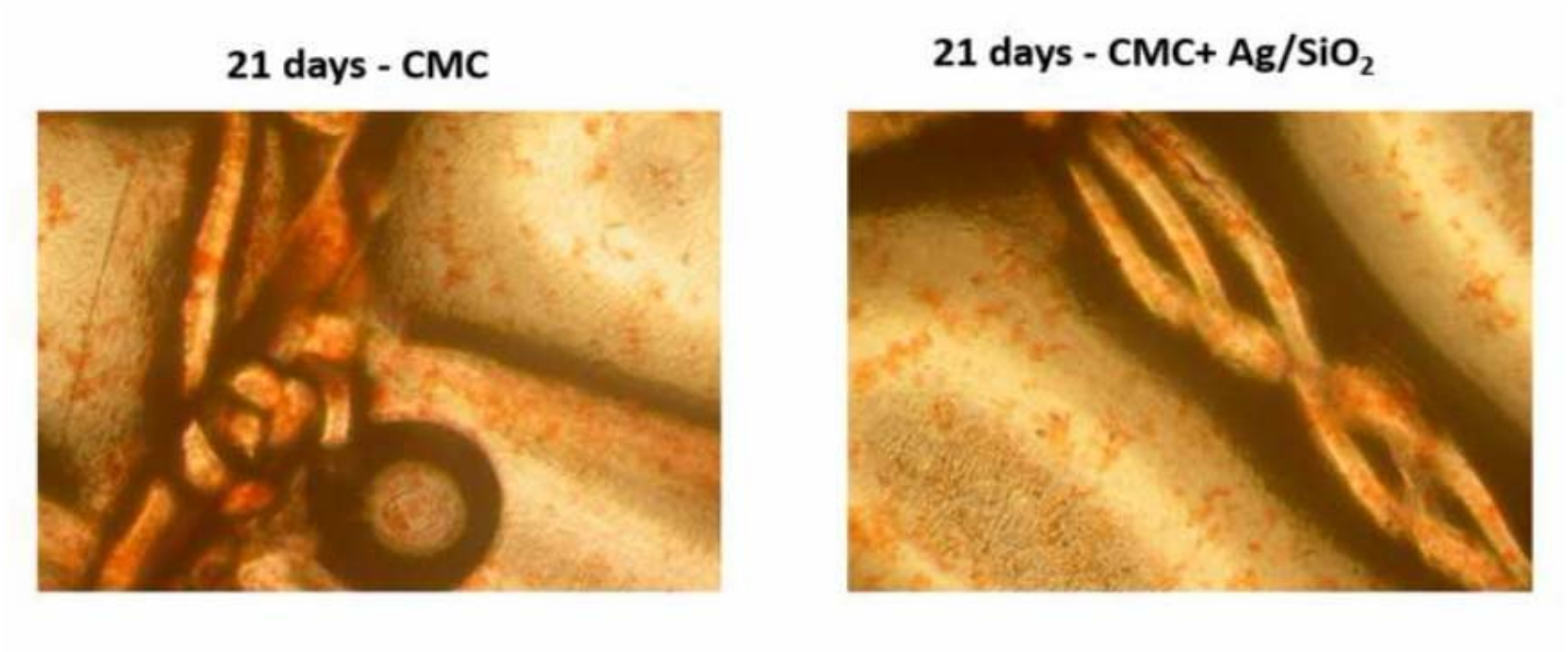

Figure 7

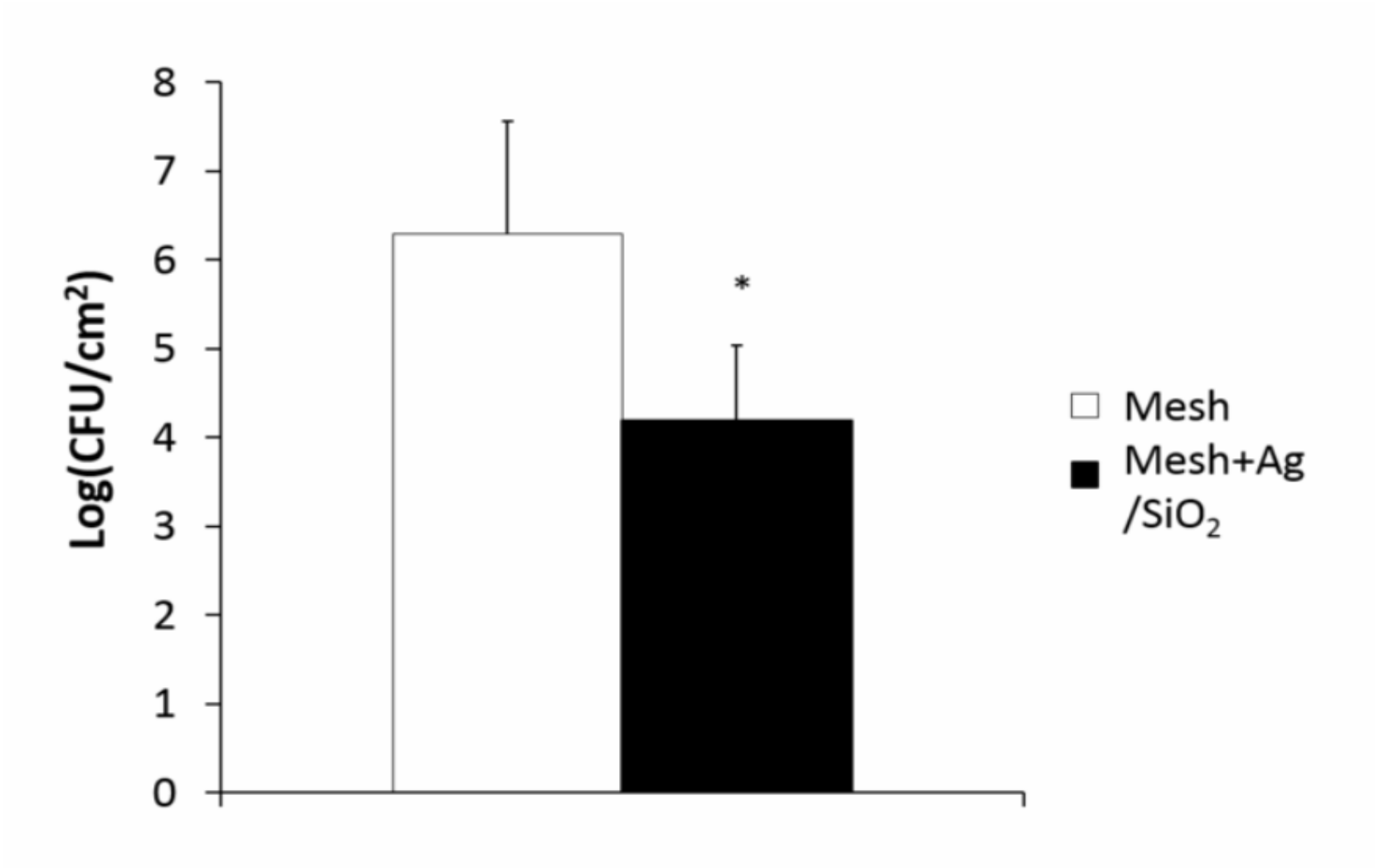

Figure 8

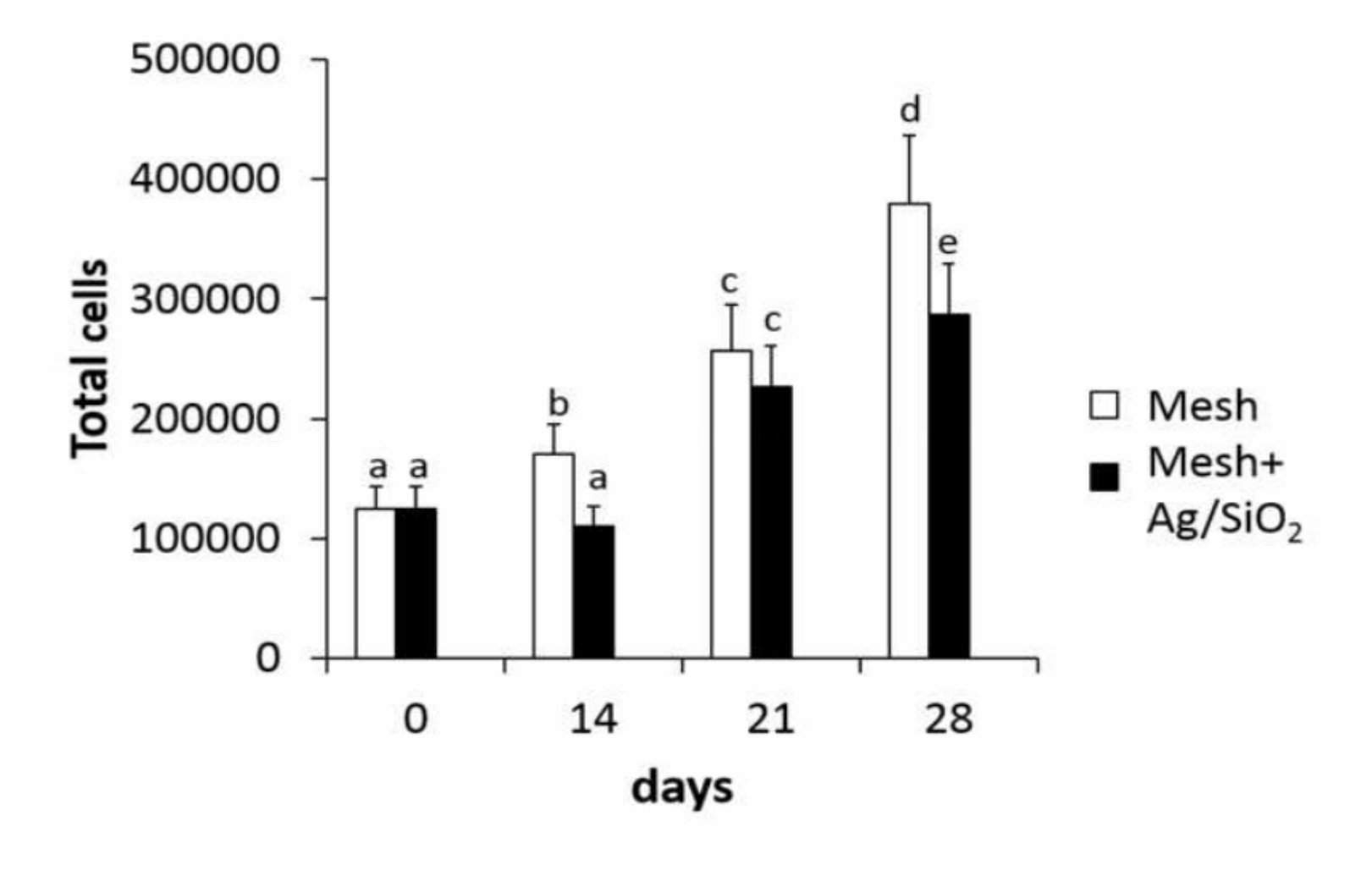
500000
400000
300000
200000
100000
0
Total cells
a a
b
a
c
c
d
e
0
14
21
28
days
Mesh
Mesh+
Ag/SiO2

Figure 9

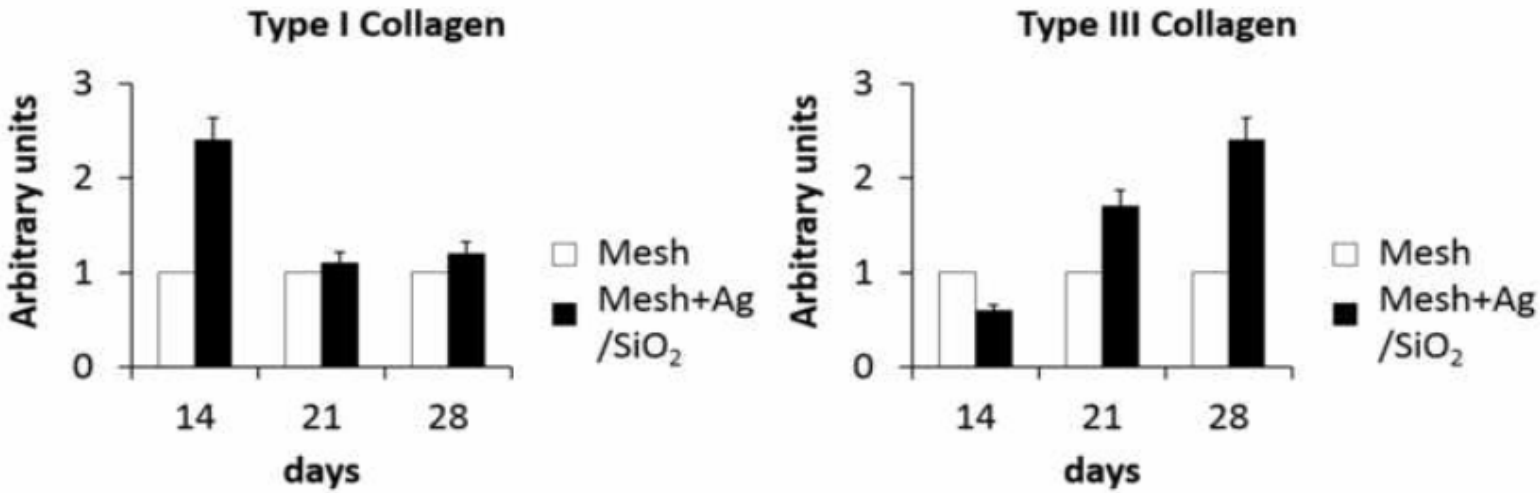
Type I Collagen
Arbitrary units
3
2
1
0
14
21
28
days
Mesh
Mesh+Ag /SiO2
Type III Collagen
Arbitrary units
3
2
1
0
14
21
28
days
Mesh
Mesh+Ag /SiO2

Figure 10

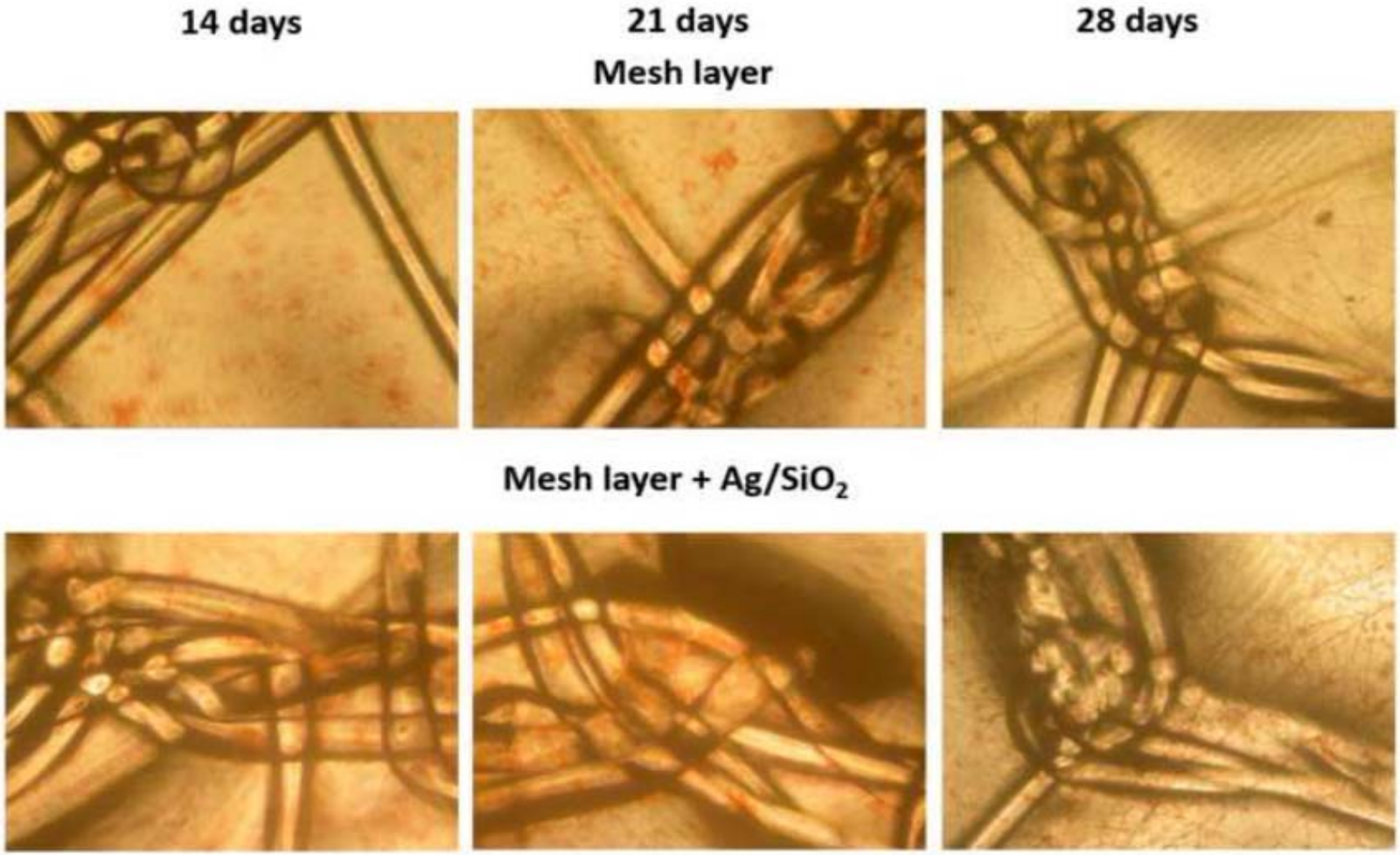

Figure 11

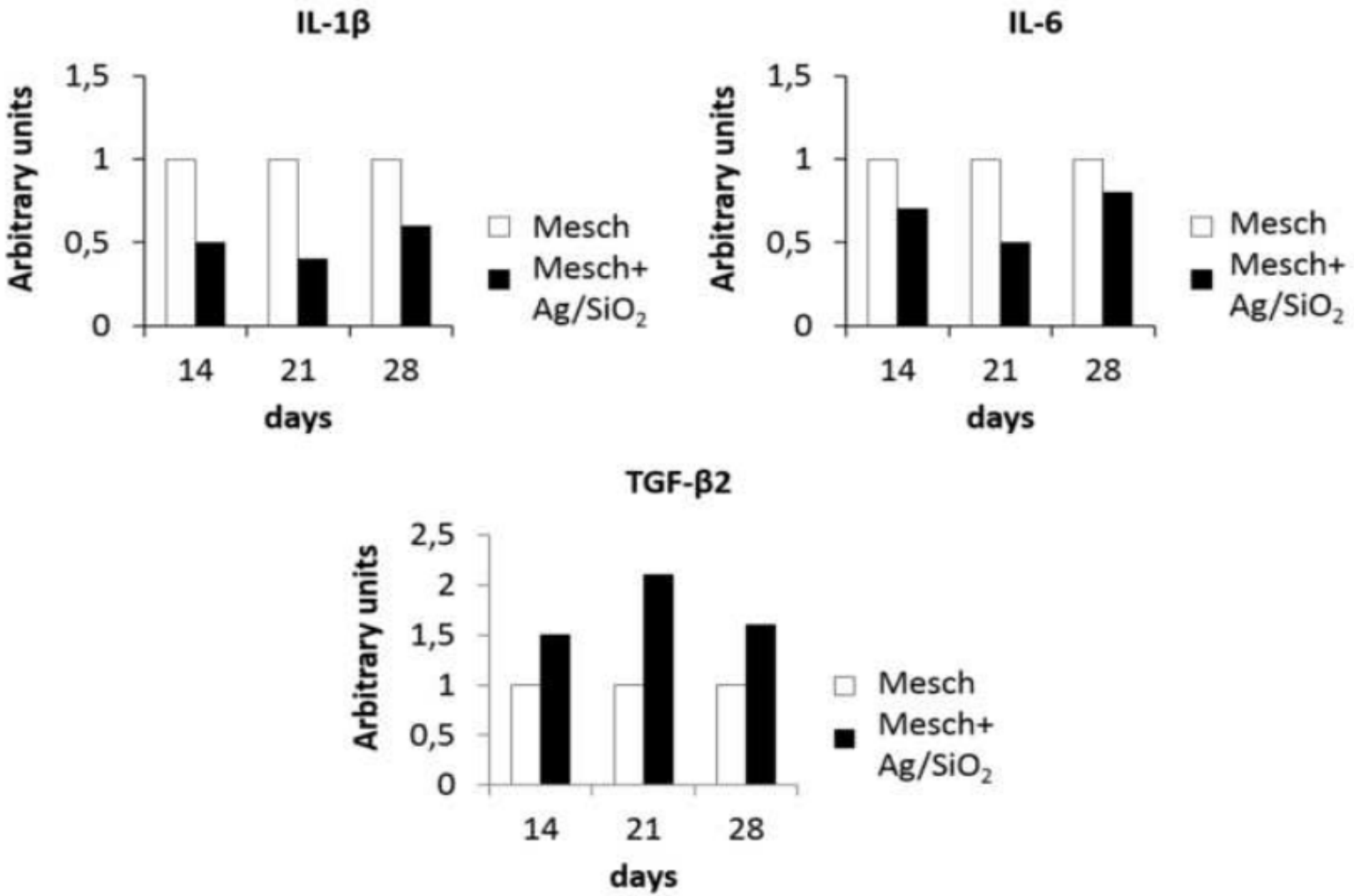
IL-1β
Arbitrary units
1,5
1
0,5
0
14
21
28
days
Mesch
Mesch+ Ag/SiO2
IL-6
Arbitrary units
1,5
1
0,5
0
14
21
28
days
Mesch
Mesch+ Ag/SiO2
TGF-β2
Arbitrary units
2,5
2
1,5
1
0,5
0
14
21
28
days
Mesch
Mesch+ Ag/SiO2

Figure 12

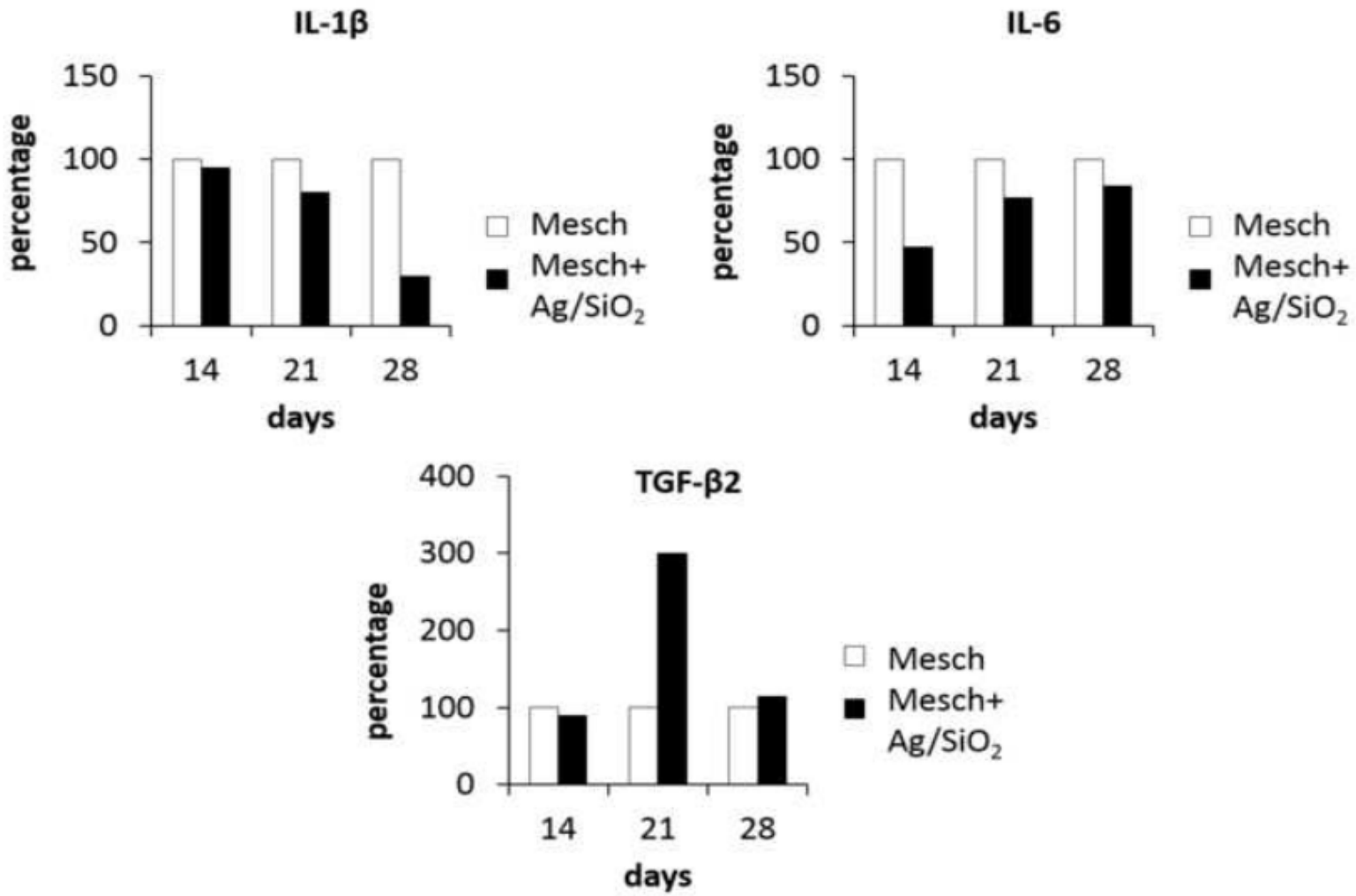
IL-1β
percentage
150
100
50
0
14
21
28
days
Mesch
Mesch+ Ag/SiO2
IL-6
percentage
150
100
50
0
14
21
28
days
Mesch
Mesch+ Ag/SiO2
TGF-β2
percentage
400
300
200
100
0
14
21
28
days
Mesch
Mesch+ Ag/SiO2